Chemical Geology, 64 (1987) 279–294
Elsevier Science Publishers B.V., Amsterdam — Printed in The Netherlands

[4]

BEHAVIOUR OF REE DURING THERMAL METAMORPHISM AND HYDROTHERMAL INFILTRATION ASSOCIATED WITH SKARN AND VEIN-TYPE TUNGSTEN ORE BODIES IN CENTRAL MOROCCO*

G. GIULIANI[1], A. CHEILLETZ[1] and M. MECHICHE[2]

[1]*Centre de Recherches Pétrographiques et Géochimiques, CRPG, F-54501, Vandoeuvre-lès-Nancy Cédex (France)*
[2]*Société Minière du Djebel Aouam, SMA, Casablanca (Morocco)*

(Received February 18, 1987; revised and accepted April 7, 1987)

Abstract

Giuliani, G., Cheilletz, A. and Mechiche, M., 1987. Behaviour of REE during thermal metamorphism and hydrothermal infiltration associated with skarn and vein-type tungsten ore bodies in central Morocco. Chem. Geol., 64: 279–294.

The analysis of REE in tungsten ore bodies and surrounding rocks from Paleozoic schist–sandstone and limestone series in central Morocco shows two kinds of behaviour: (1) no significant modification of lanthanide distribution occurs during thermal and hydrothermal metamorphic events; and (2) important variations of REE patterns characterize highly infiltrated and mineralized samples corresponding to the mixing of scheelite and wall-rock spectra. A water/rock ratio of ~2.4 is estimated for the paleogeothermal continental system. By comparison of REE patterns, hydrothermal mineralizing fluids are assumed to be derived from blind evolved late acidic magmas rather than from outcropping Aouam granitic stocks.

1. Introduction

The understanding of the geochemical behaviour of rare-earth elements (REE) in petrogenetic processes has benefited from a rather simple behaviour which may be modelled by simple laws of mass-balance and equilibrium partitioning (Schnetzler and Philpotts, 1968, 1970; Nagasawa, 1970; Cullers and Medaris, 1973; Hanson, 1978). The use of REE in the petrogenesis of magmatic rocks gives good results when applied to basalt genesis (Gast, 1968) but the interpretation of REE patterns is more difficult when dealing with the evolution of granitic series (Cocherie, 1978). The problem appears even more complicated when metamorphism and/or hydrothermal alteration processes participate in the rock history. The mobility of REE is still a matter of debate; they were largely considered as immobile during metamorphism and alteration (Green et al., 1972; O'Nions and Pankhurst, 1974; Condie et al., 1977) whereas other studies suggest a significant mobility during hydrothermal fluid circulation (Wood et al., 1976; Martin et al., 1978; Hellman et al., 1979; Alderton et al., 1980;

*Contribution C.R.P.G. No. 711.

0009-2541/87/$03.50

Mitropoulos, 1982; Leroy, 1984; Maruejol and Cuney, 1985). Illustrating this debate, while the recent study of Michard et al. (1984) deduced from direct analysis of pulses of hot waters from the East Pacific Rise during the hydrothermal interaction process that the exchange of REE is negligible, Baker and De Groot (1983) and Baker (1985) demonstrated high REE mobility during granite alteration or interaction between seawater and felsic volcanic series.

In fact, experimental studies and models have shown that REE mobility depends on very high water/rock (or magma) ratios and the presence of efficient complexing anions (carbonate, phosphate, fluoride) in the solution (Cullers and Medaris, 1973; Flynn and Burnham, 1978; Shaw, 1978; Bilal et al., 1979; Taylor and Fryer, 1983).

The debate about REE mobility largely rests on the definition of "mobility" especially when adressing the problem of REE mobility in a hydrous environment (metamorphism and/or hydrothermal alteration). Several very fundamental questions arise:

(1) How well do we know the geochemical characteristics of the untransformed parent material in terms of major- and trace-element contents including REE?

(2) If REE variations are observed, are they really attributable to interaction with the same hydrous phase which caused the other changes of the chemistry and mineralogy of the system?

(3) How well do we know the relative importance of matrix modifications and REE movements?

(4) What are the quantitative conditions of hydrothermal process (water/rock ratio, T, pH, Eh, alkalinity and complexing agents, etc)?

This paper attempts to interpret the evolution of REE distribution in tungsten ore bodies controlled by contact metamorphic processes and hot hydrothermal fluid circulation. The Djebel Aouam district offers an opportunity to study both the utilization of REE in analyzing complex hydrous alteration processes and the problem of hydrothermal REE mobility.

2. Geological setting

The Djebel Aouam mining district in central Morocco (Fig. 1) represents a complex of Hercynian geothermal systems with superimposed phases of hydrothermal activity associated with the emplacement of three small granitic stocks. This W–Pb–Zn–Ag mining district is part of the W–Sn–Mo Moroccan province and is related to post-tectonic Hercynian granitic plutons (Agard et al., 1980). The main sedimentary, tectonic, magmatic and hydrothermal events of the Djebel Aouam district (Agard et al., 1958; Cheilletz, 1983a, b) are listed in Table I.

The sedimentary rocks are mostly anchi- to epizonally metamorphosed Upper Ordovician to Lower Devonian folded series, unconformably overlain by Upper Visean sediments. A late folding and thrust faulting phase gave rise to the present general structures with a generally NE–SW strike, dipping N70–80°NW. Three small granitic stocks labelled "Mispickel", "Mine" and "Kaolin" (Fig. 1) have been assigned to an intracontinental calc-alkaline magmatic series and are associated with late-tectonic fracturing and shearing movements (Cheilletz, 1983a). These intrusives are surrounded by a large alteration halo with two superimposed phases of metamorphic transformation, the first phase being contact metamorphism (Agard et al., 1958) and the second, a hydrothermal metamorphic phase associated with the deposition of tungsten ores (Cheilletz and Isnard, 1985). The three phenomena were shown by the K–Ar method on minerals and whole rocks to have occurred at 286 ± 2 Ma (Cheilletz and Zimmermann, 1982).

2.1. Sedimentary rocks

The lower lithostratigraphic unit (François et al., 1986), the Ordovician flysch, consists of interbedded schists and sandstones topped by a layer of quartzite. Silurian schists interbedded with marl and limestone are overlain by Devonian schists and limestones (Fig. 1).

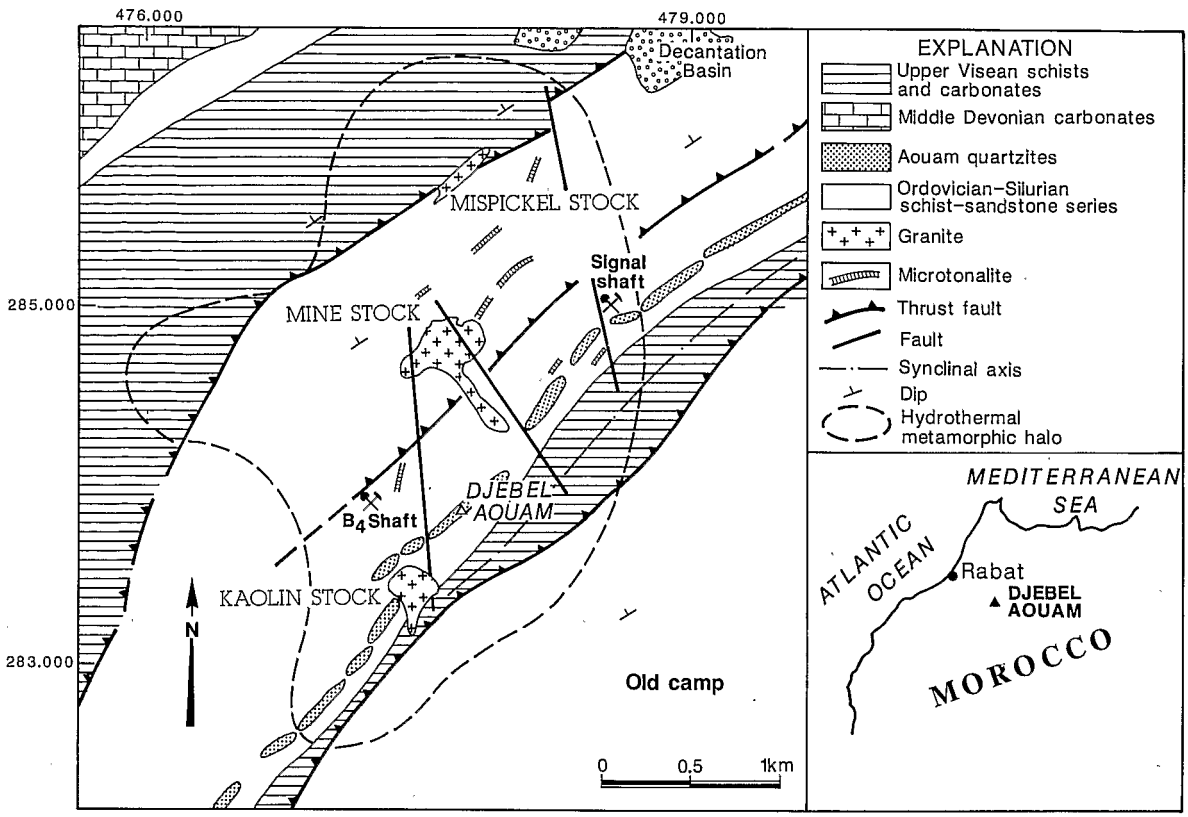

Fig. 1. Geological map of the Djebel Aouam district. The hydrothermal metamorphic halo encloses all the tungsten occurrences now detected. *Signal* and B_4 shaft are related to Pb–Zn–Ag mining exploitation.

Upper Visean conglomerates, schists and limestones mark the end of the sedimentary cycle. Representative samples of the Ordovician and Silurian series have been selected for this study (Table II).

2.2. *Contact-metamorphosed rocks*

Ordovician and Silurian schist–sandstone series were metamorphosed to biotite hornfelses. In detail, the paragenesis involves andalusite and cordierite porphyroblasts, muscovite, K-feldspar, albite, plagioclase (oligoclase to anorthite in composition), chlorite and sulfides. Chlorite is generally associated with muscovite and results from a retrograde reaction. Six samples from this group have been selected for REE analysis (Table II). A second group consists of calc-silicate bands and lenses and are the product of thermal metamorphism of contrasting lithologies such as Silurian shales and interbedded marly limestones. Five representative samples from the calc-silicate bands have been chosen for the purpose of this study (Table II).

2.3. *Hydrothermal metamorphism and tungsten mineralization*

Hydrothermal metamorphism is associated with granite intrusion and results in tungsten mineralization located within a large halo of biotitic alteration.

2.3.1. Tungsten mineralization. Two stages associated with a specified type of tungsten mineralization have been distinguished by field work: the first corresponds to the infiltration of

TABLE I

The main sedimentary, tectonic, magmatic and hydrothermal events of the Djebel Aouam district (Cheilletz, 1983a)

	fracturing and shearing	Aouam granitoids stocks 286 ± 2 Ma	hydrothermal metamorphism: Pb–Zn–Ag mineralization; W mineralization: stratiform skarn and veins
Sedimentary break	folding *2* and thrust faulting		contact-thermal metamorphism: biotitic hornfelses and calc-silicate bands
Upper Visean conglomerate schists and limestones			
Sedimentary break	folding *1* and unconformity		
Devonian schists and limestones			
Silurian schists and interbedded limestones			
Ordovician flysch			

hydrothermal fluids in calc-silicate bands leading to the development of stratiform scheelite–biotite lenses (Cheilletz, 1983b). The resulting skarn exhibits a diablastic texture with a paragenesis of quartz, Mg-biotite, actinolite, hornblende, plagioclase, ilmenite, apatite and scheelite intergrowths.

The second stage of tungsten mineralization is represented by a wolframite–scheelite-bearing quartz vein system resulting from hydrothermal fluid circulation in an open fracture system which crosscuts the early stratiform skarn.

Subvertical veins referred to as "phlogopite–scheelite veins" with high-grade ores (up to 1% WO_3) and fluorite and spinel occur in the mining district. The relationships with the quartz vein system are not clearly defined.

2.3.2. Biotitic hydrothermal metamorphism. This metamorphism is associated with the development of an important stockwork-like network of microfractures which crosscuts the metasediments. The geochemical halo of biotitic alteration has been mapped using a discriminant statistical method by Cheilletz and Isnard (1985). The vein and veinlet system is filled with quartz, biotite, K-feldspar, albite, apatite, chalcopyrite and scheelite assemblages. On account of the large rock volume affected by hot fluid circulation, it is suggested that this anomaly should be compared with the "biotitic alteration halo" of porphyry copper deposits (Lowell and Guilbert, 1970) or "hydrothermal metamorphism" in oceanic crust models (Spooner and Fyfe, 1973).

Seven representative samples of hydrothermally infiltrated rocks have been selected for the purpose of this study (Table II). They were taken from scheelite–biotite stratiform skarns [*753*bis(*1*), *753-5-6, 752-2*], biotitic-hornfelses veins and stockwork net (*368*a, *339*) and lastly from phlogopite veins (*501, 753-11*).

TABLE II

Petrographic and mineralogical characteristics of selected samples from the Djebel Aouam area

Sample No.		Petrographic identification	Mineralogical composition
605-4	sedimentary samples	quartz arenite	clastic elements: Qz, F
1		quartz wake	matrix: Ch, Mu, Kl
681		shale	accessories: Th, Zn, Ti Fe
816		impure limestone	Cc, Qz, Ch, Ti Fe
368b3	biotite hornfelses	spotted hornfels	Qz, Bi, Mu, Ilm, FK, Pl, Hm, Py, Cpy
825		muscovite hornfels	Qz, Mu, Ch, Cm, TiFe
485		biotite hornfels	Qz, Bi, Ilm, Mu, FK, Ab
541		spotted hornfels	Qz, Bi, Ch, Mu, Ilm
329		andalusite hornfels	And, Bi, Qz, Mu, Pl, Ilm, Ch
824		biotite hornfels	Qz, Bi, Mu, Ch, Ilm, Cc
644	calc-silicate bands	biotite-plagioclase zone	Bi, An, Qz, Sph, Ilm, Act HB, Mu, Ch, FK, Pyrr, Cpy, Py
404 E		biotite-plagioclase zone	Bi, An, Qz, Ilm, Act HB, Sph, Mn, Ch, Cc, FK
828		amphibole-biotite zone	Act HB, Qz, Bi, An, FeDi, Ilm, FK, Mu, Ch, Pyrr, Cpy
*368*cbf		biotite-plagioclase zone	Bi, An, Qz, FK, Ilm, Sph, Mu, Pyrr
753.9		amphibole-pyroxene zone	Act HB, FeDi, An, Qz, Bi, FK, Ab, Ch, Mu, Pyrr, Py
*753*bis(*1*)	biotitic	scheelite-biotite stratiform skarn	An, Qz, Ilm, Sph, Ch, Bi, Sc, Pyrr, Py
753-5-6	hydrothermal	scheelite-biotite stratiform	Bi, Qz, An, MgHB, Sph, Ap, FK, Mu, Ch, Sc, Ilm, Ep
752-2	metamorphism	scheelite-biotite stratiform	Bi, Qz, An, MgHB, Sph, Ap, FK, Mu, Ch, Sc, Ilm
368-a		Bi hornfels + Qz vein	Bi, Qz, ActHB, Ap, Sc, Sph, Ilm, FK, Pyrr, Spl
339		Bi hornfels + Qz vein	Qz, Bi, Sc, W, Ap, Ilm, Ch, Mu
753-11		phlogopite vein	Ph, Qz, Ol, Sc, Ap, ActHB, Ch, Mu, FK, Zr
501		phlogopite vein	Ph, Qz, Sc, Ap, FK, F, Cc, AK

Sedimentary samples: classification of Pettijohn et al. (1972). List of abbreviations: Qz = quartz; F = feldspaths; Ch = chlorite, Mu = muscovite; Kl = kaolinite, Tn = tourmaline; Zr = zircon, TiFe = Ti-Fe-oxides; Cc = calcite; Bi = biotite; Ilm = ilmenite; Pl = plagioclase; Hm = hematite; Pyr = pyrite; Cpy = Chalcopyrite; Pyrr = pyrrhotite; Ab = albite; And = andalusite; An = anorthite; ActHB = actinolite hornblende; Sph = sphene; FeDi = iron diopside; Sc = scheelite; MgHB = magnesian hornblende; Ap = apatite; Ep = epidote; Spl = sphalerite; W = wolframite; Ol = oligoclase; F = fluorine.

2.4. Granitic rocks

They are granodioritic to granitic in composition and exhibit equigranular to porphyritic textures. Microtonalite and microgranite veins complete the plutonic group of rocks. Representative analyses are listed in Table III.

3. Analytical procedure

Powder from individual skarn zones was prepared by using a drill (0.7 cm in diameter), whereas scheelite crystals were separated by grinding and hand-picking under ultraviolet light. REE analyses were performed on an ICP Jobin Yvon® *48* P spectrometer with a detection limit at twice the chondritic abundance (Govindaraju et al., 1976). Semi-quantitative microprobe analyses of individual scheelite crystals were carried out on a CAMEBAX® electron microprobe apparatus. FeO, MgO, CaO and MnO were analyzed using program correction with synthetic standards minerals. The MoO_3 content in scheelite crystals was determined by colorimetry. Major-element analysis on whole-rock samples was obtained by emission spectroscopy (Govindaraju, 1965). W and F contents in whole-rock samples were determined by colorimetry and anion-specific electrode method, respectively.

TABLE III

Major-, trace- and rare-earth-element analyses of Djebel Aouam granitoidic rocks

Rock	Microtonalite		Kaolin granodiorite		Mispickel granodiorite		Mine granite			
Sample	AM *521*	AM *542*	AM *833*	AM *402*	AM *422*	AM *320.2*	AM *302*	AM *521*b	AM *352*	AM *406*
Major oxides (wt.%):										
SiO_2	66.74	63.91	65.32	68.85	69.40	68.24	70.54	69.91	70.29	70.0
Al_2O_3	15.81	16.05	15.82	14.68	15.23	14.51	14.11	14.88	13.76	15.01
Fe_2O_3 (total)	4.45	5.80	3.91	3.17	2.65	3.53	2.90	2.57	2.77	2.61
MnO	0.04	0.07	0.05	0.06	0.01	0.06	0.02	–	0.03	–
MgO	1.85	2.43	1.85	1.26	1.25	1.37	1.00	1.19	1.06	0.87
CaO	3.55	4.49	2.99	2.12	3.15	2.79	2.03	2.09	1.81	2.40
Na_2O	3.78	2.71	3.66	3.48	2.98	3.19	3.34	3.39	3.46	3.65
K_2O	2.45	2.52	3.25	3.46	3.55	3.10	4.15	4.08	4.02	3.94
TiO_2	0.75	0.93	0.64	0.41	0.50	0.49	0.36	0.50	0.34	0.46
P_2O_5	0.11	0.26	0.09	0.14	0.16	0.16	0.05	0.09	0.03	0.18
LOI	0.90	1.01	1.36	2.79	1.15	1.37	1.02	1.40	1.61	0.80
Total	100.13	100.18	98.94	100.42	100.03	98.81	99.52	100.10	99.18	99.92
Trace elements (ppm):										
W	102	1.7	15.7	53	14.7	11.6	405	79.5	3.7	30
B	20	20	n.a.	20	20	24	20	20	20	20
Mo	1	1.5	n.a.	1	1	1	1	1	1	1
F (%)	0.10	0.06	n.a.	0.05	0.21	0.09	0.09	0.09	0.06	0.06
Cl	398	654	n.a.	52	1.90	188	466	220	255	457
S (%)	0.02	0.46	n.a.	0.18	0.11	0.02	0.16	0.04	0.11	0.11
Cu	2.5	38	n.a.	148	49	40	75	9	63	58
U	4.62	3.23	n.a.	5.32	5.59	6.58	6.37	7.72	7.67	7.59
Th	12	0.31	n.a.	14.68	13.4	12.08	15.6	15.93	15.05	16.14
La	52.06	52.96	34.07	37.48	32.24	57.89	32.14	38.79	35.90	42.66
Ce	80.83	78.03	71.04	63.91	61.51	70.48	61.31	69.53	63.00	70.51
Nd	33.62	32.57	29.18	25.22	25.74	28.89	26.32	27.86	25.29	27.93
Sm	6.35	6.29	5.82	4.63	4.48	6.04	4.68	5.32	5.09	5.33
Eu	1.30	1.48	1.26	0.97	0.88	0.90	1.09	1.01	0.92	0.93
Gd	5.07	5.07	4.05	3.56	3.52	4.72	3.86	4.22	4.00	4.20
Dy	4.00	3.27	3.21	2.54	2.64	3.14	2.83	3.30	3.31	3.23
Er	2.12	1.87	1.67	1.25	1.61	1.50	1.50	1.73	1.71	1.67
Yb	2.12	1.68	1.64	1.23	1.39	1.35	1.26	1.79	1.74	1.67
Lu	0.33	0.25	0.24	0.17	0.21	0.23	0.19	0.27	0.26	0.26
Y	23.33	n.a.	16.69	n.a.	n.a.	n.a.	n.a.	20.23	n.a.	n.a.
La/Yb	25.56	31.49	32.76	30.47	25.25	42.84	25.55	21.67	28.95	25.54

LOI = loss on ignition; n.a. = not analyzed.

4. Results

4.1. Major and trace elements

Analyses of major elements, including W and F content of selected samples from the four main petrographic groups are listed in Table IV. Chemical compositions of the different rock types have been plotted in an *ACF* diagram (Fig. 2a). The scatter reflects heterogeneity of the analyzed material. Furthermore, little chemical difference is found between schist–sandstone

TABLE IV

Major- and trace-element analyses (W, F) of Djebel Aouam district sediments and metasediments

Type	Sedimentary rocks				Biotite hornfelses					
Sample No.	*1*	*605-4*	*681*	*816*	*368b3*	*825*	*485*	*541*	*329*	*824*
SiO_2	79.60	85.51	57.28	62.71	67.85	57.56	63.05	59.55	74.38	74.57
Al_2O_3	8.83	8.15	25.30	5.93	16.41	20.03	18.54	19.85	11.92	12.37
$Fe_2O_{3\ total}$	3.53	2.68	3.10	3.96	4.58	8.27	7.10	8.24	3.93	3.38
MnO	0.07	0.02	0.02	0.17	0.06	0.06	0.12	0.13	0.05	0.05
MgO	0.90	–	1.33	0.44	1.36	2.05	1.76	1.73	1.22	1.12
CaO	0.09	–	0.6	11.74	0.98	0.54	0.36	0.65	0.94	1.37
Na_2O	0.82	0.29	0.83	1.66	1.43	1.09	0.38	1.26	2.07	2.79
K_2O	0.70	0.43	5.79	0.92	3.99	4.65	5.76	4.24	2.52	2.55
TiO_2	0.48	0.50	1.12	0.24	0.96	1.02	1.16	1.18	0.79	0.57
P_2O_5	–	0.13	0.07	0.7	0.07	–	0.17	0.34	0.44	–
LOI	2.74	2.39	5.2	10.22	2.39	5.17	1.99	3.04	1.35	0.93
Total	98.76	99.97	100.1	98.69	100.08	100.44	100.39	100.21	99.61	99.7
W (ppm)	0.9	3	2.70	2	9.5	3.1	4.6	5	2	2.6
F (%)	0.016	0.012	0.11	0.09	0.16	0.083	0.074	0.099	0.09	0.09

Type	Calc-silicate bands					Biotitic hydrothermal metamorphism						
Sample No.	*644*	*404E*	*828*	*368cbf*	*753-9*	*753bis(1)*	*753-5-6*	*752-2*	*753-11*	*368a*	*339*	*501*
SiO_2	52.90	58.96	55.36	67.77	52.37	51.91	49.75	68.91	38.55	53.63	61.83	39.70
Al_2O_3	24.98	20.99	14.31	14.09	22.15	26.72	21.19	14.95	10.35	11.47	10.34	12.62
$Fe_2O_{3\ total}$	5.42	4.08	10.74	4.77	6.05	1.23	3.50	4.19	11.42	15.59	8.11	15.41
MnO	0.05	0.06	0.18	0.05	0.1	0.02	0.05	0.04	0.19	0.08	0.08	0.13
MgO	1.70	1.01	2.06	1.37	1.6	0.27	3.11	1.71	10.39	6.71	9.48	17.55
CaO	5.60	4.69	7.35	1.89	11.76	14.83	6.42	2.68	10.74	1.41	1.44	1.66
Na_2O	3.71	2.35	1.08	4.67	0.85	1.69	4.6	3.84	1.97	0.71	0.22	0.03
K_2O	3.03	3.62	3.44	2.71	1.92	0.48	2.86	2.6	5.14	4.25	5.73	9.11
TiO_2	1.13	1.11	0.7	0.8	1.02	1.06	0.89	0.48	0.6	0.66	0.67	0.59
P_2O_5	0.16	0.07	–	0.08	0.29	0.89	0.1	0.06	0.62	0.49	0.74	–
LOI	1.78	1.6	3.63	1.32	2.37	1.23	2.2	0.92	3.28	3.86	0.99	2.90
Total	100.46	98.54	98.85	99.52	100.48	100.33	94.67	100.38	93.25	98.86	99.63	98.70
W (ppm)	26	13.9	180	3.9	10.9	205	$3.17 \cdot 10^4$	162	$4.31 \cdot 10^4$	749	$5.9 \cdot 10^3$	$1.2 \cdot 10^3$
F (%)	0.0052	0.093	0.099	0.064	0.13	0.057	0.28	0.11	0.95	1.03	n.a.	2.02

LOI = loss on ignition; n.a. = not analyzed.

samples and their metamorphosed equivalents; metamorphic reactions between interbedded carbonaceous and pelitic layers which make the calc-silicate bands (Korzhinskii, 1965, 1968; Vidale, 1969) lead to compositions falling in the biotite–anorthite–tremolite field, i.e. intermediate between the extreme initial compositions. These contrasted metamorphic rocks result as a bimetasomatic exchange by diffusion of chemical components (mainly Si^{3+}, Ca^{2+}, Fe^{2+}, Mg^{2+}) by a fluid in the intergranular spaces (Orville, 1969; Thompson, 1975).

The circulation of mineralizing fluids in metamorphic rocks is demonstrated by tungsten contents reaching >1% (Table IV). A substantial concentration of fluorine is present in the phlogopite vein sample *501*. Fig. 2b depicts the major geochemical characteristics

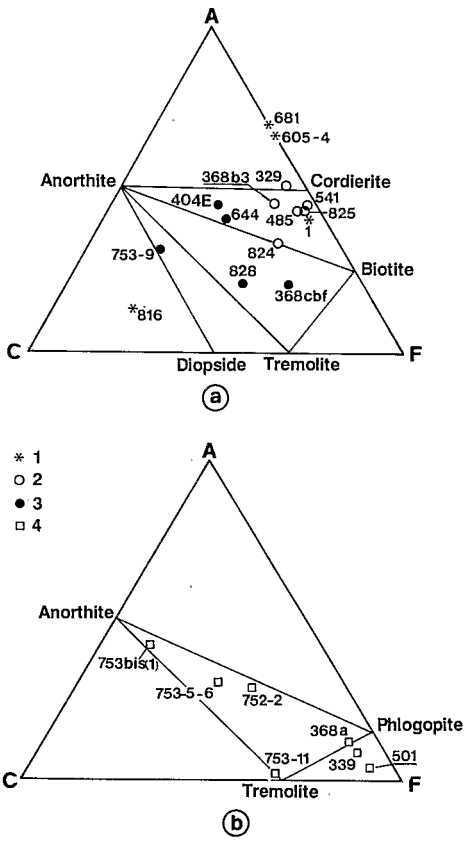

Fig. 2. a. *A* ($Al_2O_3+Na_2O+K_2O$ in molar proportions)–*C* (CaO)–*F* (FeO+MgO+MnO) triangle for the sedimentary (*1*) and contact-metamorphosed rocks: biotitic hornfelses (*2*) and calc-silicate bands (*3*).
b. *ACF* triangle for biotitic hydrothermally metamorphosed rocks (*4*).

of these samples that fall into the phlogopite–anorthite–tremolite field and accentuates the important geochemical transformations related to the hydrothermal metamorphism. The high P_2O_5 content of hydrothermally infiltrated samples (averaging 0.5% in five samples) reflects the presence of apatite. Scheelite samples (Table V) from a mineralized calc-silicate band (sample *753-11*) and quartz–biotite muscovite veins (samples *385, 496*) are virtually Mo-free in agreement with their fluorescence property. Mo-free scheelite characterizes low f_{O_2} environments (Hsu and Galli, 1973); from a stability analysis of pyrrhotite–ilmenite and ferrotremolite, oxygen fugacity during

TABLE V

Microprobe (W, Ca, Fe, Mn, Mg) and colorimetric (Mo) analyses of scheelite crystals from the Djebel Aouam

	753-11	*385*	*496*
WO_3 (%)	79.96	80.00	80.95
CaO	19.91	19.69	19.05
FeO	–	–	–
MnO	–	–	–
MgO	–	–	–
MoO_3	–	–	–
Total	99.89	99.69	100.0

753-11 = phlogopite vein; *385, 496* = quartz–biotite–muscovite veins.

scheelite crystallization has been estimated (A. Cheilletz and G. Giuliani, unpublished results, 1985) to be $\sim 10^{-19}$ atm. at 550°C.

4.2. Rare-earth elements (REE)

REE analyses of samples from the four petrographic groups, scheelite and granite are listed in Tables III and VI.

4.2.1. Sedimentary rocks. REE patterns of Djebel Aouam sedimentary rocks are represented in Fig. 3a together with the North American Shale Composite (NASC; Gromet et al., 1984) for reference; a LREE/HREE enrichment is observed with a small Eu anomaly (average $Eu/Eu^{\star}=0.68$) and $8.6<La/Yb<16.98$.

4.2.2. Biotite hornfelses and calc-silicate bands. Biotite hornfelses (Fig. 3b) and calc-silicate bands (Fig. 3c) show the same REE patterns as sedimentary rocks. The Eu anomaly is relatively constant (average $Eu/Eu^{\star}=0.75$), as is the La/Yb ratio ($15.5<La/Yb<16.5$). REE ratios between biotite hornfelses, calc-silicate bands and sedimentary rocks (Fig. 4a) show very little modification through thermal metamorphism and the variable patterns probably result from the use of only one unmodified impure limestone (*816*) as the standard for comparison.

TABLE VI

REE analysis of Djebel Aouam sediments and metasediments

Type	Sedimentary rocks				Biotite hornfelses						Calc-silicate bands				
Sample No.	*1*	*605-4*	*681*	*816*	*368*b3	*825*	*485*	*541*	*329*	*824*	*644*	*404*E	*828*	*368*cbf	*753.9*
La (ppm)	25.38	43.49	62.32	24.50	29.56	71.67	68.52	74.71	37.68	30.87	51.92	34.14	48.87	27.27	31.83
Ce	44.82	93.74	118.52	60.71	60.79	121.62	129.40	136.67	64.83	64.55	104.30	64.99	89.59	55.59	63.13
Nd	35.17	36.44	53.53	26.23	24.83	52.80	48.15	51.78	26.06	29.52	46.41	28.86	38.20	23.07	24.56
Sm	7.87	8.86	10.83	6.37	4.60	11.82	10.71	11.48	4.88	6.73	8.95	6.52	8.33	4.54	4.96
Eu	1.72	2.4	2.13	1.83	0.98	1.90	2.28	2.51	0.97	1.51	1.92	1.55	1.95	1.00	1.41
Gd	5.86	7.36	7.72	5.83	3.04	9.00	8.80	9.34	3.38	5.44	6.62	5.48	6.96	3.22	4.28
Dy	4.27	4.92	6.52	5.86	2.62	7.00	6.95	7.37	2.91	4.47	5.62	5.01	5.74	2.77	3.73
Er	1.81	2.63	3.47	3.06	1.62	3.60	3.68	4.03	1.90	2.17	2.96	2.66	2.91	1.65	1.93
Yb	1.69	2.76	3.67	2.85	2.03	3.63	3.84	4.28	2.17	2.16	3.00	2.85	2.88	1.97	1.84
Lu	0.23	0.51	0.53	0.41	0.32	0.64	0.63	0.71	0.38	0.33	0.46	0.45	0.44	0.34	0.27
Y	20.91	32.67	44.07	39.02	17.50	37.17	48.19	52.88	18.65	24.21	2.85	32.60	38.88	18.30	20.91
ΣREE	128.82	202.75	269.24	137.65	130.39	283.68	282.96	302.88	153.16	147.75	232.16	153.51	205.87	121.42	137.94
Eu/Eu*	0.76	0.67	0.60	0.68	0.80	0.55	0.80	0.71	0.74	0.76	0.73	0.76	0.77	0.73	0.93
La/Yb	15.01	15.76	16.98	8.6	14.56	19.74	17.84	17.46	17.36	14.29	17.31	11.98	16.97	13.84	17.30

Type	Biotitic hydrothermal metamorphism							Scheelite		
Sample No.	*753*bis(*1*)	*753-5-6*	*752-2*	*753-11*	*368*a	*339*	*501*	*753-11*	*385*	*496*
La (ppm)	37.91	26.01	27.92	19.94	26.76	32.51	11.29	17.59	110.36	31.22
Ce	79.19	72.55	55.03	65.05	58.55	57.58	24.03	78.61	436.06	138.89
Nd	34.35	42.69	20.98	45.35	21.45	25.82	11.35	60.96	314.74	96.92
Sm	7.58	12.54	3.91	13.26	5.09	6.96	2.27	17.76	87.45	28.76
Eu	1.44	1.13	0.76	0.68	0.95	0.59	0.19	0.46	3.76	0.59
Gd	5.85	11.25	3.22	12.74	4.82	7.60	2.34	16.62	75.44	23.52
Dy	4.73	11.45	2.78	12.53	3.76	6.82	2.07	15.26	92.04	30.09
Er	2.50	5.22	1.38	6.04	2.07	3.08	1.20	7.15	45.16	14.90
Yb	2.46	5.04	1.34	5.62	1.96	2.77	1.07	6.13	42.87	14.49
Lu	0.38	0.66	0.19	0.75	0.34	0.41	0.17	0.75	5.10	1.68
Y	26.30	58.50	17.72	72.27	27.62	42.66	13.13	78.79	497.20	149.02
ΣREE	176.39	188.54	117.51	181.96	125.75	144.14	59.98	220.99	1212.98	381.06
Eu/Eu*	0.65	0.31	0.57	0.08	0.57	0.25	0.26	0.08	0.14	0.07
La/Yb	15.41	5.16	20.84	3.55	13.65	11.74	10.55	2.87	2.57	2.16

4.2.3. Hydrothermal infiltration. Hydrothermal infiltration samples (Fig. 3d) show two kinds of REE patterns:

(1) Samples *753*bis(*1*), *368*a and *752-2* present a general REE pattern similar to that of sedimentary and thermal metamorphic rocks, i.e. with a LREE/HREE enrichment ($13.7 < La/Yb < 20.8$) and with a small Eu anomaly ($0.57 < Eu/Eu^{*} < 0.67$); the tungsten grade ranges from 162 to 749 ppm (Table IV).

(2) Samples *753-5-6* and *753-11*, *339* and *501* show important differences in REE distribution due to the existence of a large Eu anomaly ($0.08 < Eu/Eu^{*} < 0.31$) and a lower relative enrichment of LREE ($3.55 < La/Yb < 11.74$). Sample *501* also exhibits this kind of REE spectrum with a decrease in total REE content (ΣREE analyzed = 60 ppm); the highest tungsten grade occurs in these rocks ($0.12\% < W < 4.31\%$).

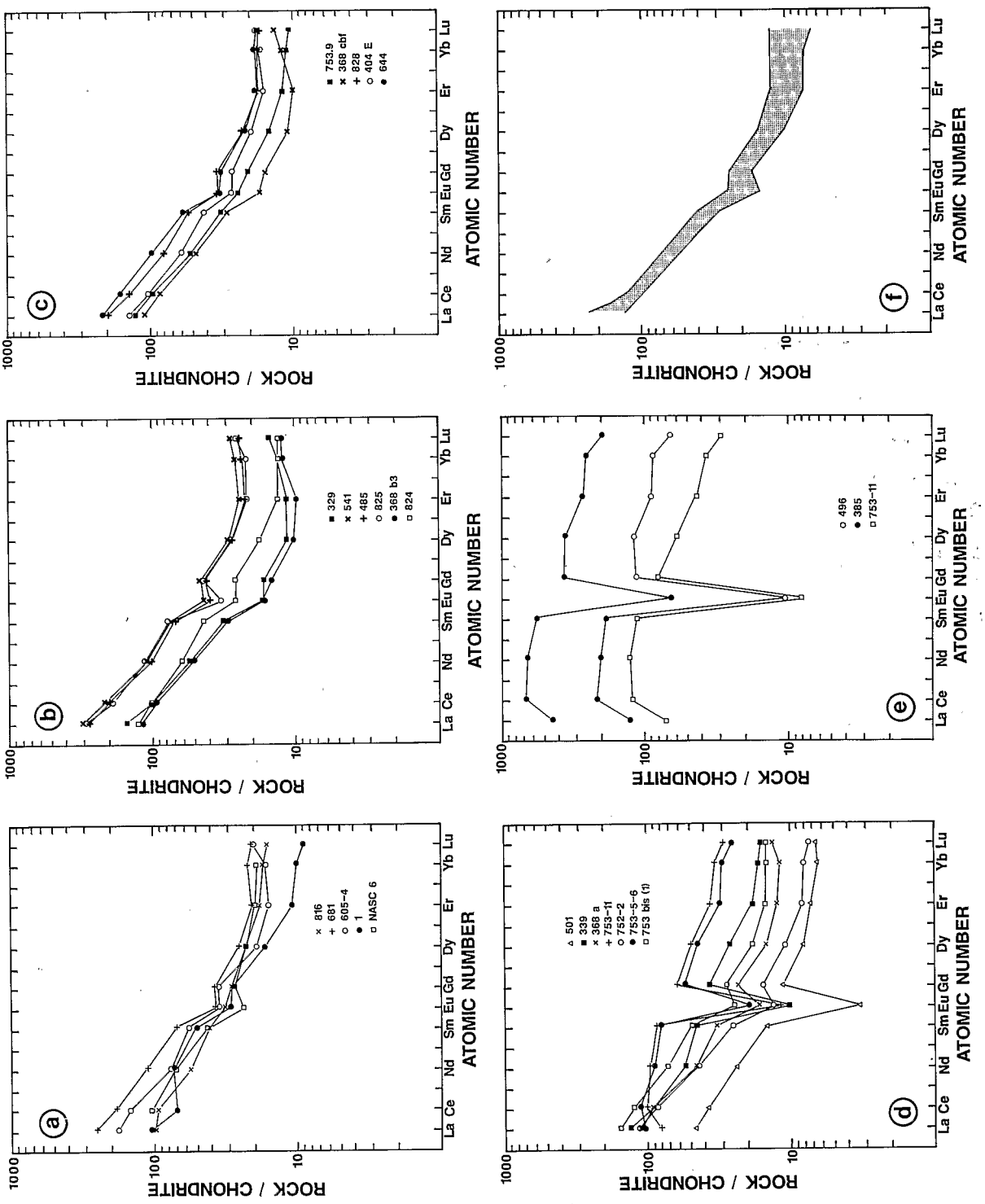
a
× 816
+ 681
○ 605-4
● 1
□ NASC 6
b
■ 329
× 541
+ 485
○ 825
● 368 b3
□ 824
c
■ 753.9
× 368 cbf
+ 828
○ 404 E
● 644
d
△ 501
■ 339
× 368 a
+ 753-11
○ 752-2
● 753-5-6
□ 753 bis (1)
e
○ 496
● 385
□ 753-11
f
ROCK / CHONDRITE
1000
100
10
La Ce Nd Sm Eu Gd Dy Er Yb Lu
ATOMIC NUMBER

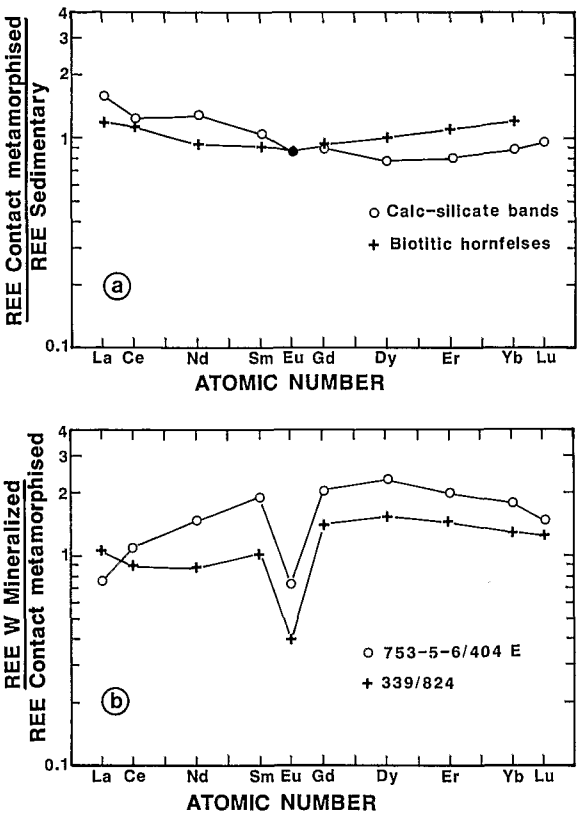

Fig. 4. a. Ratio of the average REE content in metamorphosed and unmetamorphosed sediments.
b. Ratio of the REE content in representative W-mineralized samples and their metamorphic equivalent. See Table VI for sample identification.

Similar modifications are seen on a REE ratio diagram (Fig. 4b) between selected mineralized samples and their untransformed equivalent. Compared to the biotitic hornfelses (*824*), the mineralized vein sample (*339*) exhibits a small LREE decrease, moderate HREE enrichment and a strong Eu anomaly; a similar modification of HREE and Eu content is shown between the calc-silicate band (*404*E) and scheelite skarn lens (*753-5-6*), but here moderate LREE enrichment occurs.

4.2.4. Scheelite. Purified samples of scheelite (Fig. 3e) present a rather flat REE pattern ($2.16 < La/Yb < 2.87$) with a large negative Eu anomaly ($0.07 < Eu/Eu^{\star} < 0.14$); so-called "bird spectra aspect". The total REE amount appears quite variable but high (221 ppm $< \sum REE <$ 1213 ppm; 436 ppm Ce in sample *385*) with depletion of La.

4.2.5. Granites. Granodioritic rocks show the same REE patterns as microtonalites and microgranites (Fig. 3f), and the enrichment of REE is 45–60 times that of the chondrites. The REE spectra appear fractionated ($21.7 < La/Yb < 43$) with small Eu anomalies. The REE spectra of Djebel Aouam plutonic rocks present a typical calc-alkaline shape (Gromet et al., 1984).

5. Discussion

This study of the REE changes accompanying the tungsten mineralization in sedimentary and metasedimentary rocks clearly demonstrates that the distribution of REE in highly altered rocks is completely dependent on REE patterns of accessory phases such as scheelite. This effect may be reinforced by the presence of apatite which presents coefficients of REE partitioning between W and magma or W and hydrothermal fluid close to those of scheelite (Nagasawa, 1970; Cottrant, 1981; Raimbault, 1985). This effect of accessory minerals on REE patterns (which may be assimilated to the "grain effect" phenomenon) has already been demonstrated in other petrological examples

Fig. 3. a. REE patterns of sediments. NASC (*6*) from Gromet et al. (1984, p. 2471). Chondrite-normalized values from Evensen et al. (1978).
b. REE patterns for biotitic hornfelses.
c. REE patterns for calc-silicate bands.
d. REE patterns of metasediment-bearing hydrothermal biotite.
e. REE patterns for scheelite crystals.
f. REE patterns of granitic rocks from Djebel Aouam district.

(Towell et al., 1965; Nagasawa, 1970; Condie et al., 1977; Exley, 1980; Fourcade and Allègre, 1981; Charoy, 1986).

Exact mass-balance calculations of the metamorphic and hydrothermal transformations taking account of the distribution of major and trace elements appear rather difficult. A major problem occurs in estimating the geochemical characteristics of the rocks prior to their metamorphic and hydrothermal alteration. In the case of the Djebel Aouam district, this problem is aggravated by the great variety of initial lithologies (Table II; Fig. 2) showing poor stratigraphic correlation between unmetamorphosed and metamorphosed zones. For these reasons REE distributions will not be considered in the frame of a general mass-balance calculation and the problem will be approached by considering global distribution and by comparing each set of samples.

Variations in REE patterns during thermal and hydrothermal events appear to be characterized by two distinct types of behaviour:

(1) No change may be ascribed to contact metamorphism resulting in the formation of biotitic hornfelses and calc-silicate bands in spite of important mineralogical and chemical modifications of the original sedimentary rocks. This result agrees with previous works (Mitropoulos, 1982; Cathelineau, 1985) and confirms that REE patterns and abundances in metamorphosed rocks may be used to identify the nature of original sediments in a metamorphic environment.

(2) In contrast, hydrothermally infiltrated rocks show significant REE pattern variations: the Eu anomaly (Fig. 5a) and the La/Yb ratio (Fig. 5b) have been plotted against tungsten content as an indicator of hydrothermal fluid circulation: the Eu anomaly becomes more and more negative, HREE/LREE fractionation decreases and the spectra converge towards those of scheelite. The Eu anomaly becomes very pronounced only above 1000 ppm W. This result confirms the immobile character of REE during metamorphism and hydrothermal alteration processes except along zones of intense circulation correlated with potential economic concentrations. The same conclusion may be drawn from Fig. 5b: the progressive increase in W corresponds to a decrease in the La/Yb ratio with a general trend consistent with scheelite addition.

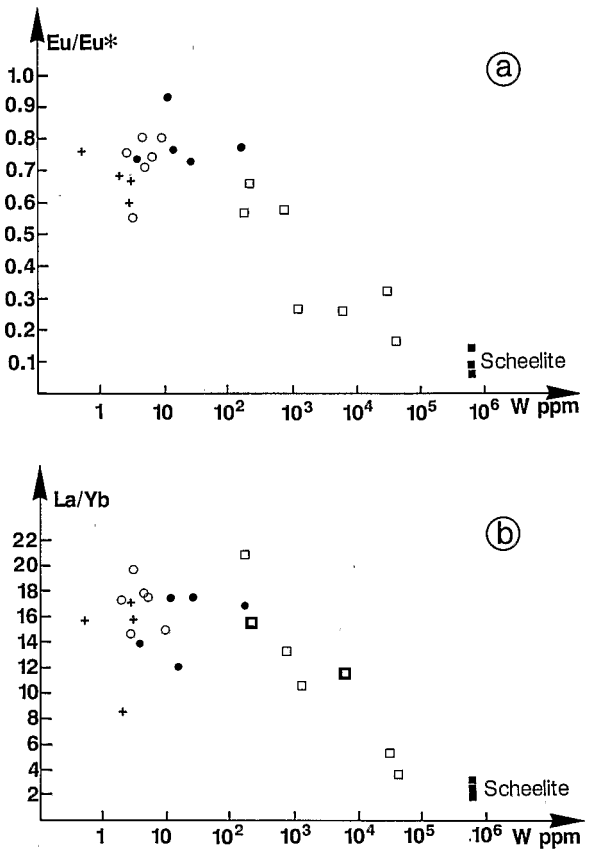

Fig. 5. a. Eu anomaly vs. W diagram for the four petrographic groups from Djebel Aouam area including scheelite analyses (*solid square*). For other *symbols*, see Fig. 2.
b. La/Yb vs. W diagram for the four petrographic groups. The good correlation between scheelite analyses and hydrothermally transformed samples represents a trend of scheelite addition. For *solid square* see (a); for other *symbols*, see Fig. 2.

Approximate calculations of fluid/rock ratios during hydrothermal circulation may be performed using experimental data on scheelite solubility (Foster, 1977) and analytical results from Djebel Aouam tungsten occurrences (Cheilletz, 1984; A. Cheilletz and G. Giuliani,

unpublished data, 1985). As stated previously, visible modifications of REE spectra are produced by fluid circulation corresponding roughly to an addition of 1000 ppm W, i.e. a scheelite/rock ratio of 1565. Temperature, pressure and salinity of the hydrothermal fluids which precipitated the Djebel Aouam tungsten ores are estimated at 400–600°C, 1–1.8 kbar and salinity 6–18 eq. wt.% NaCl, respectively. Assuming saturation of the hydrothermal fluid in these conditions, i.e. a scheelite/fluid ratio of 650 (Foster, 1977) it is possible to calculate a water/rock ratio of ~2.4. Such a value is in the range of water/rock ratios determined for active marine geothermal systems, i.e. 1.5–5 (Edmond et al., 1982; Michard et al., 1984). Therefore the modifications of REE patterns appear related to the amount of hydrothermal fluid circulations in an open fracture system.

A few experimental and calculated scheelite/fluid partition coefficients for the temperature range of our example are now available (Cottrant, 1981; Raimbault, 1985). These are very high, estimated at 4400 for Lu and 28,000 for La (Raimbault, 1985). The coefficients imply almost complete extraction of the REE from the hydrothermal fluid by the scheelite crystals in closed precipitation conditions. It is therefore suggested that, within a constant factor, REE spectra of scheelite mimic those of the parent hydrothermal fluids.

REE may also be used to elucidate the origin of the mineralizing fluids. Because of the geological relationships of the three small granitic stocks with the mineralized halo, a link between these granites and tungsten ore might be suspected. However, the low fluid/magma REE partition coefficient experimentally determined (Flynn and Burnham, 1978) and the great discrepancy between the spectra of Djebel Aouam granites REE and that of hydrothermal fluids implies a distinct origin for these fluids.

In fact, some similarities may be found between the REE patterns of Djebel Aouam scheelite and the products of late magmatic differentiation in various plutonic associations such as the calc-alkaline complex of Querigut, Pyrénées (Fourcade and Allègre, 1981), adamellite of Xihuashan (Le Bel et al., 1984), Western Corsica association (Cocherie et al., 1985, 1987), peraluminous series of South Mountain batholith, Nova Scotia (Muecke and Clarke, 1981), Manaslu leucogranite from Nepal (Vidal et al., 1982), Sweetwater Wash pluton from California (Mittlefehldt and Miller, 1983), alkali-feldspar granites as Bärhalde granite (Emmermann et al., 1975) and peraluminous pegmatitic granites of Wennipeg River district (Goad and Černý, 1981). The REE spectra of these rocks are characterized especially by a huge negative Eu anomaly and $(La/Yb)_N \simeq 1$, hence suggesting genetic relationships between Djebel Aouam tungsten mineralizations and late acidic magmatic history.

Moreover, W deposition in the Djebel Aouam area is accompanied by an important large-ion lithophile element (LILE) and halogen metasomatism with K, Rb, Na, F and Cl enrichment in the alteration halo (Cheilletz and Isnard, 1985). The concentration of these elements is known to occur during various igneous differentiation processes; their final stages lead to late acid magmatic bodies with marked geochemical characteristics especially concerning REE distribution.

The interpretation of the highly negative Eu anomaly characterizing the REE distribution in scheelites from skarns, phlogopite veins and quartz veins raises some difficulties particularly because of the dependance of the Eu partition coefficient on the Eu^{2+}/Eu^{3+} ratio of the solution. In the Lacoste area (Southern Massif Central, France), similar REE spectra with large negative Eu anomalies in scheelite have been interpreted as resulting from crystal growth in reducing conditions (Guion et al., 1985) as suggested for the Djebel Aouam Mo-free scheelites.

6. Conclusions

No significant modification of lanthanide distribution in sedimentary rocks occurs during

contact and weak hydrothermal metamorphism, leading to the development of biotitic hornfelses and calc-silicate bands.

On the contrary, extensive variations of REE patterns occur in hydrothermally infiltrated rocks, characterized by the development of a negative Eu anomaly and a decrease in the La/Yb fractionation ratio. These variations result from the mixing of the REE spectra of scheelite and metamorphic surrounding rocks. A 1000-ppm W enrichment in infiltrated wall rocks seems necessary to produce a visible modification of REE spectra.

REE pattern analysis demonstrates also that scheelite and related hydrothermal fluids cannot be derived from the known Djebel Aouam granites but rather from evolved late acidic magmas. This conclusion does not require a direct magmatic origin for the mineralizing fluids but more likely some sort of long-lasting equilibration; stable-isotope studies probably may help to clarify this. The present model places the source of tungsten at depth and predicts the existence of blind granitic bodies beneath the Djebel Aouam area.

Acknowledgements

This paper has benefitted of large corrections by F. Albarède, B. Charoy and J.M. Montel (CRPG) and Ian Mc Reath (Universidade Federal da Bahia, Salvador, Brazil). K. Govindaraju, M. Vernet and J.M. Claude undertook the chemical and physical analyses. Illustrations were drawn by A. Legros and A.L. Montéragioni typed the manuscript. C. Devey and R. Duda helped with the English translation.

References

Agard, J., Balcon, J.M. and Morin, Ph., 1958. Étude géologique et métallogénique de la région minéralisée du Jbel Aouam (Maroc Central). Notes Mém. Serv. Géol. Maroc, No. 132, 126 pp.

Agard, J., Emberger, A. and Moussa, S., 1980. Les unités métallogéniques du Maroc. Notes Mém. Serv. Géol. Maroc, 276: 37–59.

Alderton, D.H.M., Pearce, J.A. and Potts, P.J., 1980. Rare-earth element mobility during granite alteration: Evidence from southwest England. Earth Planet. Sci. Lett., 49: 149–165.

Baker, J.H., 1985. Rare earth and other trace element mobility accompanying albitization in a Proterozoic granite, west Bergslagen, Sweden. Mineral. Mag., 49: 107–115.

Baker, J.H. and De Groot, P.A., 1983. Proterozoic seawater–felsic volcanics interaction, west Bergslagen, Sweden — Evidence for high REE mobility and implications for 1.8 Ga seawater compositions. Contrib. Mineral. Petrol., 82: 119–130.

Bilal, B.A., Herrmann, F. and Fleisher, W., 1979. Complex formation of trace elements in geochemical systems, 1. Potentiometric study of fluor-complexes of rare elements in fluorite-bearing model system. J. Inorg. Nucl. Chem., 40: 347–350.

Cathelineau, M., 1985. Behavior of rare-earth elements during alteration of a volcanic calc-alkaline series (Los Azufres geothermal system, Mexico). Terra Cognita, 5(2–3): 193 (abstract).

Charoy, B., 1986. The genesis of the Cornubian batholith (South-West England): The example of the Carnmenellis pluton. J. Petrol., 27: 571–604.

Cheilletz, A., 1983a. Le contrôle structural des minéralisations filoniennes en tungstène du Djebel Aouam, Maroc Central: application au système filonien Plomb–Zinc–Argent. C.R. Acad. Sci., Paris, 297: 417–420.

Cheilletz, A., 1983b. Les lentilles rubannées stratiformes à scheelite–biotite du Djebel Aouam, Maroc Central. Première description et interprétation. C.R. Acad. Sci., Paris, 297: 581–584.

Cheilletz, A., 1984. Caractéristiques géochimiques et thermobarométriques des fluides associés à la scheelite et au quartz des minéralisations de tungstène du Jbel Aouam (Maroc Central). Bull. Minéral., 107: 255–272.

Cheilletz, A. and Isnard, P., 1985. Contribution à la prospection des gisements hydrothermaux de tungstène sur l'exemple du district polymétallique W–Pb–Zn–Ag du Jbel Aouam (Maroc Central). Miner. Deposita, 20: 220–230.

Cheilletz, A. and Zimmermann, J.L., 1982. Datations par la méthode K–Ar du complexe intrusif et des minéralisations en tungstène du Jbel Aouam (Maroc Central). C.R. Acad. Sci., Paris, Sér. II, 295: 255–258.

Cocherie, A., 1978. Géochimie des Terres Rares dans les granitoïdes. Thesis, University of Rennes, Rennes, 116 pp.

Cocherie, A., Rossi, P. and Le Bel, L., 1985. The Variscan calc-alkalic plutonism of western Corsica: Mineralogy and major- and trace-element geochemistry. Rapp. Bur. Rech. Géol. Min.-Group. Int. Sci., Orléans, 19 pp.

Cocherie, A., Rossi, P. and Le Bel, L., 1987. The Variscan calc-alkalic plutonism of western Corsica: Mineralogy

and major and trace element geochemistry. Phys. Earth Planet. Inter., 45: 145–178.

Condie, K.C., Viljoen, M.J. and Kable, E.J.D., 1977. Effects of alteration on element distributions in Archean tholeiites from the Barberton Greenstone Belt, South Africa. Contrib. Mineral. Petrol., 64: 75–89.

Cottrant, J.F., 1981. Cristallochimie et géochimie des terres rares dans la scheelite. Application à quelques gisements français. Thesis, University of Paris VI, Paris, 99 pp.

Cullers, R.L. and Medaris, G., 1973. Experimental studies of the distribution of rare earths as trace elements among silicate minerals and liquids and water. Geochim. Cosmochim. Acta, 37: 1499–1512.

Edmond, J.M., von Damm, K.L., McDuff, R.E. and Measures, C.I., 1982. Chemistry of hot springs on the East Pacific Rise and their effluent dispersal. Nature (London), 297: 187.

Emmermann, R., Daieva, L. and Schneider, J., 1975. Petrologic significance of rare earth distribution in granites. Contrib. Mineral. Petrol., 52: 267–283.

Evensen, N.M., Hamilton, P.J. and O'Nions, R.K., 1978. Rare-earth abundances in chondritic meteorites. Geochim. Cosmochim. Acta, 42: 1199–1212.

Exley, R.A., 1980. Microprobe studies of REE-rich accessory minerals: implications for Skye granite petrogenesis and REE mobility in hydrothermal systems. Earth Planet. Sci. Lett., 48: 97–110.

Flynn, R.T. and Burnham, C.W., 1978. An experimental determination of rare-earth partition coefficients between a chloride containing vapor phase and silicate melts. Geochim. Cosmochim. Acta, 42: 685–701.

Foster, R.P., 1977. Solubility of scheelite in hydrothermal chloride solutions. Chem. Geol., 20: 27–43.

Fourcade, S. and Allègre, C.J., 1981. Trace elements behavior in granite genesis: A case study of the calc-alkaline plutonic association from the Querigut Complex (Pyrénées, France). Contrib. Mineral. Petrol., 76: 177–195.

François, J.M., Regnault, S. and Cheilletz, A., 1986. Mise au point concernant les séries de l'Ordovicien-Silurien-Devonien inférieur du Djebel Aouam (Maroc Central). Bull. Soc. Géol. Fr., 2: 293–297.

Gast, P.W., 1968. Trace element fractionation and the origin of tholeitic and alkaline magma types. Geochim. Cosmochim. Acta, 32: 1057–1086.

Goad, B.E. and Černý, P., 1981. Peraluminous pegmatitic granites and their pegmatite aureoles in the Winnipeg River district, Southeastern Manitoba. Can. Mineral., 19: 177–194.

Govindaraju, K., 1965. Dosage des éléments majeurs et roches silicatées par spectrométrie photoélectrique avec le quantomètre ARL. Bull. Soc. Fr. Céram., 67: 25–43.

Govindaraju, K., Mevelle, G. and Chouard, C., 1976. Automated optical emission spectrochemical bulk analysis of silicate rocks with microwave plasma excitation. Anal. Chem., 48: 1325–1331.

Green, T.H., Brunfelt, A.O. and Heier, K.S., 1972. Rare-earth element distribution and K/Rb ratios in granulites, mangerites and anorthosites, Lofoten–Vesteraalen, Norway. Geochim. Cosmochim. Acta, 36: 241–257.

Gromet, L.P., Dymek, R.F., Haskin, L.A. and Korotev, R.L., 1984. The "North American shale composite": Its compilation major and trace element characteristics. Geochim. Cosmochim. Acta, 48: 2469–2482.

Guion, J.L., Touray, J.C., Joron, J.L. and Tollon, F., 1985. Détermination de l'état de valence prédominant de l'europium en solutions hydrothermales à partir des spectres de terres rares de couples scheelite–feldspath: Application au district de Montredon (Tarn). Bull. Minéral., 108: 855–858.

Hanson, G.N., 1978. The application of trace elements to the petrogenesis of igneous rocks of granitic composition. Earth. Planet. Sci. Lett., 38: 26–43.

Hellman, P.L., Smith, R.E. and Henderson, P., 1979. The mobility of the rare earth elements: Evidence and implications from selected terrains affected by burial metamorphism. Contrib. Mineral. Petrol., 71: 23–44.

Hsu, L.C. and Galli, P.E., 1973. Origin of the scheelite-powellite series of minerals. Econ. Geol., 68: 681–696.

Korzhinskii, D.S., 1965. The theory of systems with perfectly mobile components and processes of mineral formation. Am. J. Sci., 263: 193–205.

Korzhinskii, D.S., 1968. The theory of metasomatic zoning. Miner. Deposita, 3: 222–231.

Le Bel, L., Li, Yi-dou and Sheng, Ji-fou, 1984. Granitic evolution of the Xihuashan–Dangping (Jiangxi, China). Tschermaks Mineral. Petrogr. Mitt., 33: 149–167.

Leroy, J., 1984. Comportement du thorium et des terres rares lors de phénomènes hydrothermaux et supergènes en environnement granitique: exemple des gisements d'uranium du Nord-Ouest du Massif Central. Bull. Liaison S.F.M.C., 107-5: 82–83.

Lowell, J.D. and Guilbert, J.M., 1970. Lateral and vertical alteration mineralization zoning in porphyry ore deposits. Econ. Geol., 65: 373–408.

Martin, R.F., Whitley, J.E. and Woolley, A.R., 1978. An investigation of rare-earth mobility: fenitized quartzites, Borralan Complex, N.W. Scotland. Contrib. Mineral. Petrol., 66: 69–73.

Maruejol, P. and Cuney, M., 1985. Xihuashan, tungsten-bearing granites (Tiangxi, China): mineralogical controls on REE, Y, Th, U mobility during magmatic evolution and hydrothermal alteration. Terra Cognita, 5(2-3): 284 (abstract).

Michard, G., Albarède, F., Michard, A., Minster, J.-F., Charlot, J.-L. and Tan, N., 1984. Chemistry of solutions from the 13°N East Pacific Rise hydrothermal site. Earth Planet. Sci. Lett., 67: 297–307.

Mitropoulos, P., 1982. REE patterns of the metasedimentary rocks of the Land's End granite aureole (southwest England). Chem. Geol., 35: 265–280.

Mittlefehldt, D.W. and Miller, C.F., 1983. Geochemistry of the Sweetwater Wash Pluton, California: Implications for "anomalous" trace-element behavior during differentiation of felsic magmas. Geochim. Cosmochim. Acta, 47: 109–124.

Muecke, G.K. and Clarke, D.B., 1981. Geochemical evolution of the South Mountain batholith, Nova Scotia: Rare-earth-element evidence. Can. Mineral., 19: 133–145.

Nagasawa, H., 1970. Rare-earth concentrations in zircons and apatites and their host dacites and granites. Earth Planet. Sci. Lett., 9: 359–364.

O'Nions, R.K. and Pankhurst, R.J., 1974. Rare-earth element distribution in Archaean gneisses and anorthosites, Godthåb area, West Greenland. Earth Planet. Sci. Lett., 22: 328–338.

Orville, P.M., 1969. A model for metamorphic differentiation origin of thin-layered amphibolites. Am. J. Sci., 267: 64–86.

Pettijohn, F.J., Potter, P.E. and Siever, R., 1972. Sand and Sandstone. Springer, New York, N.Y., 618 pp.

Raimbault, L., 1985. Utilisation des spectres de terres rares des minéraux hydrothermaux (apatite, fluorine, scheelite, wolframite) pour la caractérisation des fluides minéralisateurs et l'identification des magmas sources et des processus évolutifs. Bull. Minéral., 108: 737–744.

Schnetzler, C.C. and Philpotts, J.A., 1968. Partition coefficients of rare-earth elements and barium between igneous matrix material and rock-forming-mineral phenocrysts. I. In: L.H. Ahrens (Editor), Origin and Distribution of the Elements. Pergamon, New York, N.Y., pp. 929–938.

Schnetzler, C.C. and Philpotts, J.A., 1970. Partition coefficients of rare-earth elements between igneous matrix material and rock-forming mineral phenocrysts, II. Geochim. Cosmochim. Acta, 34: 331–340.

Shaw, D.M., 1978. Trace element behaviour during anatexis in the presence of a fluid phase. Geochim. Cosmochim. Acta, 42: 933–943.

Spooner, E.T.C. and Fyfe, W.S., 1973. Sub-sea-floor metamorphism, heat and mass transfer. Contrib. Mineral. Petrol., 42: 287–304.

Taylor, R.P. and Fryer, B.J., 1983. Rare earth element lithogeochemistry of granitoid mineral deposits. Rare Earth Geochem., 76: 74–84.

Thompson, A.B., 1975. Calc-silicate diffusion zones between marble and pelitic schist. J. Petrol., 16: 314–346.

Towell, D.G., Winchester, J.W. and Volfovsky Spirn, R., 1965. Rare-earth distribution in some rocks and associted minerals of the batholith of Southern California. J. Geophys. Res., 70: 3485–3496.

Vidal, Ph., Cocherie, A. and Le Fort, P., 1982. Geochemical investigations of the origin of the Manaslu leucogranite (Himalaya, Nepal). Geochim. Cosmochim. Acta, 46: 2279–2292.

Vidale, R., 1969. Metasomatism in a chemical gradient and the formation of calc-silicate bands. Am. J. Sci., 267: 857–874.

Wood, D.A., Gibson, I.L. and Thompson, R.N., 1976. Elemental mobility during zeolite facies metamorphism of the Tertiary basalts of eastern Iceland. Contrib. Mineral. Petrol., 55: 241–254.